Published in final edited form as:
Neuroimage. 2011 July 1; 57(1): 182–189. doi:10.1016/j.neuroimage.2011.03.060.

Early Time Points Perfusion Imaging: Theoretical Analysis of Correction Factors for relative cerebral blood flow Estimation Given Local Arterial Input Function

Kenneth K. Kwong[1,*] and **David A. Chesler**[1]

[1] MGH/MIT/HMS Athinoula A. Martinos Center for Biomedical Imaging, Department of Radiology, Massachusetts General Hospital, Charlestown, MA 02129, USA

Abstract

If local arterial input function (AIF) could be identified, we present a theoretical approach to generate a correction factor based on local AIF for the estimation of relative cerebral blood flow (rCBF) under the framework of early time points perfusion imaging (ET). If $C(t)$, the contrast agent bolus concentration signal time course, is used for rCBF estimation in ET, the correction factor for $C(t)$ is the integral of its local AIF. The recipe to apply the correction factor is to divide $C(t)$ by the integral of its local AIF to obtain the correct rCBF. By similar analysis, the correction factor for the maximum derivative (MD1) of $C(t)$ is the maximum signal of AIF and the correction factor for the maximum second derivative (MD2) of $C(t)$ is the maximum derivative of AIF. In the specific case of using normalized gamma-variate function as a model for AIF, the correction factor for $C(t)$ (but not for MD1) at the time to reach the maximum derivative is relatively insensitive to the shape of the local AIF.

Keywords

local arterial input function (local AIF); dynamic susceptibility contrast-enhanced magnetic resonance imaging; early time points (ET) perfusion imaging method; incomplete gamma function; gamma-variate function model; correction factors

Introduction

What ET can do if local AIF can be found

Dynamic imaging of a bolus of contrast agent passing through the brain's vascular system is the basis for the formation of tissue bolus signal time courses and of the arterial input function (AIF). In routine clinical data analysis, global AIF is assumed even though local AIF is reasonably expected. Identifying local AIF accurately (Calamante, 2005; Calamante et al., 2000; Lorenz et al., 2006a; Lorenz et al., 2006b; Willats et al., 2006, 2008) remains a great technical challenge. Methods to identify local AIF's will not be investigated in this manuscript. Instead, we investigate the case of what the early time points perfusion imaging

*Corresponding Author: Kenneth K Kwong, MGH-NMR Center, 149 - 13th Street (Mailcode 2301), Charlestown, MA 02129, USA, Tel: +1-617-724-9519, kwong@nmr.mgh.harvard.edu.

(ET) method (Kwong et al., 2011) can do under the condition of local AIF's already being identified. In other words, how can ET, which has assumed global AIF previously, utilize that given local AIF information to make meaningful relative cerebral blood flow (rCBF) maps? We provide in this manuscript a theoretical recipe to utilize local AIF information to generate correction factors for rCBF estimation by ET.

It should be mentioned that in ET, the analysis of rCBF given a number of identifiable local AIF's in one single individual is equivalent to the analysis of rCBF given different global AIF's for different individuals. In ET, AIF is needed for cross-subject comparison but obtaining global AIF for each individual is straight forward. As long as the problem of local AIF identification has been solved, whatever results we can learn about rCBF evaluation by ET from the investigation of the local AIF question of a single individual will be directly applicable to the question of cross-subject comparison of rCBF. For cross-subject comparison by ET, we could have also considered a reference based method similar to the reference-based maximum up-slope (Ref-US) method (Kimura and Kusahara, 2009) which requires setting a region of interest (ROI) on some referential tissue (e.g. white matter ROI) but would not require any AIF information. Since the focus of this manuscript is on local AIF analysis which could not be helped by the reference-based method (except in the unlikely and inconvenient scenario that one can find a similar reference tissue ROI at each brain region supplied by a local AIF), we will not pursue the reference-based topic here.

Subtopic: Is the rCBF result obtained by the maximum gradient based method independent of local AIF?

In the investigation of the myriad ways that can be used to estimate rCBF by ET given known local AIF information, we also obtained an answer as a byproduct of our correction factor analysis to the following interesting question: Within the framework of using the normalized gamma-variate function as a model for AIF, is the rCBF result obtained by the well established maximum gradient based method (Kimura and Kusahara, 2009; Koenig et al., 1998; Miles, 1991; Miles and Griffiths, 2003) independent of local AIF?

Different correction factors based on local AIF are required for different types of MR signal used for rCBF estimation by ET

With global AIF, rCBF can be estimated with ET by simply taking the ratio of MR signals of early time points of different voxels, eliminating the dependence of AIF altogether. Early time points are expected to be data points acquired before the tissue mean transit time T which amounts to a few seconds for gray matter in humans. With local AIF (or in cross-subject comparison), ET is no longer independent of AIF. If we want to find the relative flow of two voxels that have different AIF's, it is necessary to take into account the different shapes of the two AIF's. In other words, correction factors which vary according to the shapes of local AIF would be required for rCBF estimation by ET if local AIF's are known in advance. In addition, since ET is known for its flexibility (Kwong et al., 2011) in allowing many different ways to be used to estimate rCBF, different correction factors are also required for the many different approaches of employing ET.

Here we will identify and study the correction factors based on local AIF for three different ways to calculate rCBF with ET, each with its own justification. These three ways include the use of 1) MR signal intensity ($\Delta R2^*$) of the contrast agent bolus concentration time course, named $C(t)$ for short, at an arbitrary early time point, 2) maximum derivative of $C(t)$, named MD1 for short and 3) maximum second derivative of $C(t)$, named MD2 for short. With regard to real world experimental data, $C(t)$ is the preferred choice for rCBF evaluation due to its superior contrast to noise (CNR) but $C(t)$ can be hampered by the need to accurately identifying a reference time point for ET (Kwong et al., 2011) to correct for the

time delay of the arrival of the bolus of contrast agent. The main justification of using MD1 and MD2 over using $C(t)$ is that there is less need to accurately and explicitly identify a reference time point for ET. MD1 is of additional interest because it is linked to the traditional maximum gradient based method for perfusion analysis. The justification of using the MD2, despite its lower CNR than MD1, is that the time to reach MD1, named TMD1 for short, runs a higher risk of being longer than tissue mean transit time T. Exceeding T would mean violating ET's basic assumption of measuring the amount of contrast agent before any contrast agent leaves the tissue. For convenience in later presentation, the time to reach the maximum second derivative MD2 is also named TMD2 which is unlikely to exceed T.

These three selected ways of ET perfusion analysis would encompass a fair representation of a broad range of approaches to evaluate rCBF using ET. The study of the correction factors for these three chosen ways would provide useful examples of a recipe to generate correction factors for rCBF evaluation by ET given local AIF.

The relationship between local AIF and the bolus signal time courses C (t) in ET

The most straightforward way to look at how local AIF can affect rCBF evaluation is to look at how $C(t)$ needs to be corrected to be used to measure rCBF in ET. For simplicity, let's assume that only two local AIF's, AIF_1 and AIF_2, supply two separate regions of the brain even though the presentation in this manuscript applies to as many local AIF's as necessary. Perfusion information can be obtained from the bolus contrast agent concentration time curve in the general expression given below:

$$C(t) \approx f(AIF \otimes R(t)) \qquad \text{Eq (1)}$$

where $C(t)$ is the tissue contrast agent concentration signal (ΔR2*) time curve, f is the perfusion term, AIF is arterial input function, $\otimes$ is the convolution symbol and $R(t)$ is the residue function which is the probability that a molecule of the agent that entered the capillary bed at $t = 0$ is still there at time t (Buxton, 2002; Ostergaard et al., 1996). The ET's basic assumption is for the residue function $R(t) = 1$ and $t < T$, leading to Eq (2) below (Kwong et al., 2011) which confirms that rCBF (flow ratio) result evaluated by ET is independent of AIF (global AIF is assumed).

$$rCBF = ratio\ of\ C(t) = ratio\ of\ f \qquad \text{Eq (2)}$$

In the case of local AIF, Eq (1) can be written as,

$$C_1(t) \approx f_1(AIF_1 \otimes R(t)) \qquad \text{Eq (3a)}$$

$$C_2(t) \approx f_2(AIF_2 \otimes R(t)) \qquad \text{Eq (3b)}$$

where f_1 and f_2 represent different blood flow values and $C_1(t)$ and $C_2(t)$ are two bolus signal time courses associated with $AIF_1(t)$ and $AIF_2(t)$. When ET's basic assumption ($R(t) = 1$ and $t < T$) is met, $C(t)$ behaves like the microsphere model and the convolution term ($AIF \otimes R(t)$) of Eq (1 and 3) turns into an integral term

$$C(t) \approx f \int_0^t AIF(\tau) d\tau \quad \text{Eq (4)}$$

with $t < T$.

Methods: General Recipe

General recipe for obtaining correction factor for C(t) in the rCBF estimation by ET

From Eq (4), it can be observed immediately that the integral $\int_0^t AIF(\tau) d\tau$ can be used as a correction factor for $C(t)$ given local AIF because

$$f \approx \frac{C(t)}{\int_0^t AIF(\tau) d\tau}$$

The recipe for the correction factor for each associated AIF is simply dividing each $C(t)$ by the integral of its local AIF to obtain the correct flow value. The same time point t will be chosen for both $C(t)$ and $\int_0^t AIF(\tau) d\tau$. All the tissue bolus signal time courses $C(t)$ fed by the same local AIF_1 would pick the same time t, say t_1 to estimate their corrected flow values. Time courses $C(t)$ fed by a different AIF_2 are free to pick a different time, say t_2. In choosing the time point for rCBF estimation, it is assumed that the bolus transit delay of each $C(t)$ and $AIF(t)$ has already been corrected.

Normalization of the measured local AIF

So far the local AIF's listed in Eq 1, 3 and 4 are the "true" local AIF's which have assumed properties that the total integral under the local arterial concentration curve has the same value for all tissues in the brain (Axel, 1980; Calamante et al., 2004). "True" AIF's are unlikely to be measurable in practice. The measured AIF at a local artery is unlikely to be a duplicate of the "true" AIF due to interference such as vessel orientation, partial volume of tissues, inflow artifacts, etc. So when we are comparing measured local AIF's we are not only measuring the difference among the "true" local AIF's but also artifact-weighted MR signal of each local AIF. However, if we make the assumption that the measured AIF at least keeps the same shape of the "true" AIF, measured AIF will differ from the true AIF only by some arbitrary constant value. Taking into account the consideration of the difference among measured local AIF's, the integral term $\int_0^t AIF(\tau) d\tau$ of Eq (4) should be replaced by a normalized integral, namely an integral normalized by the total area of the measured AIF as below

$$\frac{\int_0^t AIF(\tau) d\tau}{\int_0^\infty AIF(\tau) d\tau}$$

Both the numerator (the integral of AIF up to a pre-selected time point t) and the denominator (total integral of AIF) are measureable. The normalized integral differs from $\int_0^t AIF(\tau) d\tau$ only by a constant, unique to each local AIF.

With normalization, terms in Eq (4) turn into the normalized integral $\int_0^t AIF_N(\tau)d\tau$ with

$$AIF_N(t)=\frac{AIF(t)}{\int_0^\infty AIF(\tau)d\tau}$$

and the normalized $C_N(t)$ with

$$C_N(t)=\frac{C(t)}{\int_0^\infty AIF(\tau)d\tau}$$

Since all future description and discussion of $AIF(t)$, $C(t)$ and the correction factors in this manuscript are working only with normalized terms, there is really no need to keep the cumbersome subscript N to indicate normalization. So for convenience

$AIF(t) = = AIF_N(t)$ *and* $C(t) = = C_N(t)$ from now on and Eq (4) with normalized terms would be listed again as

$$C(t) \approx f\int_0^t AIF(\tau)d\tau$$

There shouldn't be any confusion.

Pre-correction required for ET: bolus transit delay pre-correction using relative time of arrival (rTOA) of the bolus

Before $C(t)$ and local $AIF(t)$ can be used for rCBF estimation, both of them need to be corrected for transit delay before the correction term $\int_0^t AIF(\tau)d\tau$ can be usefully applied. Conceptually, obtaining the information of the time of arrival (TOA) (Kwong et al., 2011) of the contrast agent bolus is the most convenient way for ET to handle the bolus transit delay correction for $C(t)$ and local $AIF(t)$. However, as shown in the companion paper (Kwong et al.) the low CNR consideration of TOA encourages the utilization of other reference time points for ET, time points with superior CNR known collectively as relative TOA (rTOA). *In this manuscript, we will investigate the correction factors given the following rTOA*'s: the time to reach the maximum first derivative (TMD1) and the time to reach the maximum second derivative (TMD2). For all voxels given a single AIF, each rTOA retains the same respective time distance from TOA. MD1, the value of the maximum derivative, and MD2, the value of the maximum second derivative can be taken to estimate flow.

Making correction factors for C (t), MD1 and MD2 at specific rTOA's which are TMD1 and TMD2

Flow can be estimated using MD1 and MD2 without the explicit knowledge of TOA. Utilizing rTOA's, one can evaluate flow using $C(t)$ at t=TMD1 and at t=TMD2. We are presenting below the recipe for making the correction factors for $C(t)$ at TMD1 and TMD2 and the correction factors for MD1 and MD2. As mentioned above, the result of MD1 is translatable identically to the result the maximum gradient based method for perfusion analysis.

Making correction factor for C(t) at TMD1

If we take TMD1 of each $C(t)$ to be the time point to apply the correction factor in order to evaluate rCBF, the upper time limit t for the integral $\int_0^t AIF(\tau)d\tau$ would be the relative time distance between TMD1 and TOA. It is important to recognize that TMD1 of $C(t)$, in terms of its relative time distance to TOA, is the same as the time to reach the maximum signal (not the maximum derivative) of the AIF itself. The reason is that

$$\frac{d}{dt}\int_0^t AIF(\tau)d\tau = AIF(t) \qquad \text{Eq (5)}$$

according to the second fundamental theorem of Calculus. Combining Eq 4 and 5

$$\frac{d}{dt}C(t) \approx f\frac{d}{dt}\int_0^t AIF(\tau)d\tau = fAIF(t) \qquad \text{Eq (6)}$$

Therefore, relative to TOA, the time to reach the MD1, namely TMD1, is the time to reach the maximum signal of AIF.

For convenience, the time to reach the maximum signal of AIF is named TMAIF. The correction factor for the contrast agent signal intensity of C(t) at TMD1 is therefore

$$\int_0^{TMD1\ of\ C(t)} AIF(\tau)d\tau = \int_0^{TMAIF} AIF(\tau)d\tau$$

if we assume that $t = 0$ is the same as TOA. The correction factor, which is just a constant value, once found, is applied to all $C(t)$ of a particular brain region at the time point TMD1.

Now we know the upper time setting of the integral $\int_0^{TMAIF} AIF(\tau)d\tau$, how do we determine the lower time setting if we do not know TOA which should be assigned to t=0? Fortunately, we can take the integral from the time TMAIF backwards. Presumably the part of the integral that involves the baseline would be averaged to zero because if noise is present, be it random or physiological, the mean of the baseline should be zero, translating into that part of the integral becoming zero. So we could generate the correction factor without any knowledge of TOA.

Making the correction factor for MD1

Using the MD1 to calculate rCBF is simply the classical maximum gradient method for perfusion analysis and MD1 is known for its robustness (Kwong et al., 2011) appropriate for rCBF estimation. In using $\frac{d}{dt}C(t)$ for rCBF evaluation, we can derive from Eq (6)

$$f \approx \frac{\frac{d}{dt}C(t)}{\frac{d}{dt}\int_0^t AIF(\tau)d\tau}$$

or,

$$f \approx \frac{\frac{d}{dt}C(t)}{AIF(t)}$$

The correction factor is now $\frac{d}{dt}\int_0^t AIF(\tau)d\tau$ or equivalently, $AIF(t)$. At TMD1, It simply means that MD1 of each $C(t)$ should now be corrected by the maximum signal of AIF, or the value of AIF at TMAIF. Please notice the detail of the current correction factor which is now the maximum value of *AIF*, not the integral $\int_0^{TMAIF} AIF(\tau)d\tau$ listed above which is the correction factor for $C(t)$. So we have the convenient result that the correction factor for the maximum derivative is simply the maximum value of AIF.

This maximum value of AIF (also known as the height of AIF) being used for the correction factor for MD1 at TMD1 is well established in the literature of the maximum gradient based method (Axel, 1980; Herfkens et al., 1982; Kimura and Kusahara, 2009; Miles, 1991). We are just recasting it in the framework of ET.

Making the correction factor for C(t) at TMD2 and the correction factor for MD2

We have explored the correction factor for $C(t)$ at TMD1 and the correction factor for MD1 at TMD1. Since TMD1 runs a higher risk of violating ET's basic assumption (Kwong et al., 2011) than TMD2 in experimental data, it makes sense to study the correction factor when TMD2 is used as rTOA. We will demonstrate how to make the correction factor for $C(t)$ at t = TMD2 as well as the correction factor for MD2 at TMD2. Incidentally, since the value of the second derivative at TMD1 is zero, there is no point of studying the second derivative of C(t) at TMD1.

The correction factor for $C(t)$ at TMD2 is

$$\int_0^{TMD2\ of\ C(t)} AIF(\tau)d\tau = \int_0^{TMD1\ of\ AIF} AIF(\tau)d\tau$$

because relative to TOA, the time point to reach the maximum derivative of AIF is equivalent to TMD2 of $C(t)$.

The correction factor for MD2, on the other hand, is the maximum derivative value of AIF. The explanation is that

$$\frac{d^2}{dt}C(t) \approx f\frac{d^2}{dt}\int_0^t AIF(\tau)d\tau \qquad \text{Eq (7)}$$

$$\frac{d^2}{dt}C(t) \approx f\frac{d}{dt}AIF(t) \qquad \text{Eq (8)}$$

Hence,

$$f \approx \frac{\frac{d^2}{dt}C(t)}{\frac{d}{dt}AIF(t)}$$

As a generalization, to use the maximum derivative of any order *a* for rCBF estimation, the correction factor would be *the derivative* of order *a* of the integral of local AIF or equivalently the maximum derivative of the order of $a - 1$ of AIF.

Methods: Specific Modeling of local AIF

The gamma-variate function is used as a model for local AIF to showcase the correction factors

To illustrate concretely how to make correction factors based on local AIF for the purpose of evaluating rCBF by ET, we use the popular gamma-variate function as a model for AIF.

Given the gamma-variate function $e^{-t}t^{a-1}$ as a model for AIF, the correction factor $\int_0^t AIF(\tau)d\tau$, after proper normalization of the gamma-variate function, will become the incomplete lower gamma function

$$P(t,a)=\frac{1}{\Gamma(a)}\int_0^t e^{-\tau}\tau^{a-1}d\tau \qquad \text{Eq (9)}$$

Different *a* values in $e^{-t}t^{a-1}$ give us different local AIF's.

From Eq (4), we obtain

$$f \approx \frac{C(t)}{P(t,a)}$$

The values of incomplete lower gamma function $P(t, a)$ for different values of *a* can be obtained by Matlab.

A more general AIF model using the gamma-variate function yields the same results as P(t, a) at TMD1 and TMD2

Instead of using $e^{-t}t^{a-1}$ as the model for AIF, a more generalized AIF model $e^{-bt}t^{a-1}$ can be used equally well and now the correction factor $\int_0^t AIF(\tau)d\tau$ will become

$$S(t,a,b)=\frac{\int_0^t e^{-b\tau}\tau^{a-1}d\tau}{\int_0^\infty e^{-b\tau}\tau^{a-1}d\tau} \qquad \text{Eq (10)}$$

For $S(t, a, b)$, $TMD1=\frac{a-1}{b}$ and $\text{TMD2}=\frac{(a-1)-\sqrt{a-1}}{b}$. For comparison, TMD1 = $a - 1$ and TMD2=$(a - 1) - \sqrt{a-1}$ with respect to $P(t, a)$ At *t* equal to their respective TMD1 or TMD2, $S(t, a, b) = P(t, a)$. That means whatever we can demonstrate for $P(t, a)$, we obtain the same answer for $S(t, a, b)$ at their respective TMD1 or TMD2. Varying the *b* term in

$e^{-bt}t^{a-1}$ is not going to make a difference. Since we are focusing on the results of the correction factors at TMD1 and TMD2, the study of the properties of $P(t, a)$ is sufficient for our purpose.

Results from the correction factor *P*(*t*, *a*)

In the simulated time courses of local AIF, the bolus transit delay is assumed to have all been properly corrected. With future applications for experimental data in mind, we present the results of the correction factors at the designated rTOA's of TMD1 and TMD2. We compared the results of correction factors made from changing the value of a of $P(t, a)$. The values of a between 3 and 5 fall within the value range normally used for AIF modeling (Calamante et al., 2000; Wu et al., 2003a; Wu et al., 2003b). We assume that range of a values reflects what is observed in real world data.

Given a = 3,4,5 for $P(t, a)$, TMD1=$a - 1$ and TMD2=$a - 1 - \sqrt{a-1}$. Hence,

$$\text{TMD1}=2, 3, 4$$
$$\text{TMD2}=2-\sqrt{2}, 3-\sqrt{3}, 4-\sqrt{4}$$

$P(t, a)$ and $\frac{d}{dt}P(t, a)$ share the interesting and similar results that $P(t, a)$ is relatively independent of a at t =TMD1 and $\frac{d}{dt}P(t, a)$ is relatively independent of a at t =TMD2.

Results of the correction factor P(t, a) at TMD1 or TMD2 with different values of a

To evaluate f with $C(t)$, the correction factor is $P(t, a)$. Given a =3,4,5,

$$P(t, a)=0.323, 0.353, 0.371 \text{ for } t=\text{TMD1 and}$$
$$P(t, a)=0.0217, 0.04, 0.0527 \text{ for } t=\text{TMD2}$$

The example of $P(t, a)$ at t =TMD1 is demonstrated at Fig. 1a which shows that given different a's, $P(t, a)$ at TMD1 returns values relatively insensitive to a.

Results of the correction factor $\frac{d}{dt}P(t, a)$ at TMD1 or TMD2 with different values of a

To evaluate f with $\frac{d}{dt}C(t)$, the correction factor is $\frac{d}{dt}P(t, a)$. Given a = 3,4,5,

$$\frac{d}{dt}P(t, a)=0.27, 0.224, 0.195 \text{ for } t=\text{TMD1 and}$$
$$\frac{d}{dt}P(t, a)=0.0955, 0.0956, 0.0902 \text{ for } t=\text{TMD2}$$

The example of $\frac{d}{dt}P(t, a)$ for t =TMD1 is demonstrated at Fig. 1b which shows that given different a's, $\frac{d}{dt}P(t, a)$ at TMD1 returns values sensitive to a. $\frac{d}{dt}P(t, a)$ at TMD1 is just the correction factor for MD1, so MD1 is sensitive to the shape of the model AIF.

On the other hand, $\frac{d}{dt}P(t, a)$ at t =TMD2 returns values relatively insensitive to a.

Results of the correction factor $\frac{d^2}{dt}P(t, a)$ at TMD1 or TMD2 with different values of a

To evaluate f with $\frac{d^2}{dt}C(t)$, the correction factor is $\frac{d^2}{dt}P(t, a)$. Given a = 3,4,5,

$$\frac{d^2}{dt}P(t,a)=0.0 \text{ for } t=\text{TMD1 and}$$
$$\frac{d^2}{dt}P(t,a)=0.2306, 0.1306, 0, 0902 \text{ for } t=\text{TMD2}$$

Given different *a's*, $\frac{d^2}{dt}P(t,a)$ at TMD2 returns values sensitive to *a*. $\frac{d^2}{dt}P(t,a)$ at TMD2 is just the correction factor for MD2, so MD2 sensitive to the shape of the model AIF.

Results summarized

Table 1 below summarizes the result of correction factors for the three variants of the incomplete lower gamma functions at TMD1 and TMD2.

rCBF result obtained by C(t) at TMD1 is relatively insensitive to local AIF

For a=3,4,5, $P(t, a)$ = 0.323, 0.353, 0.371 at TMD1. The difference between $P(t, 3)$ and $P(t, 4)$ at TMD1 is 8% and that between $P(t, 4)$ and $P(t, 5)$ at TMD1 is less than 5%. That suggests that the correction factor for $C(t)$ is relatively insensitive to *a*, or of the shape of the AIF. That is also the case for the correction factor $\frac{d}{dt}P(t,a)$ at TMD2. The error of $\frac{d}{dt}P(t,a)$ is less than 1% for *a* between 3 and 4 and around 5% for *a* between 4 and 5. That suggests that if $C(t)$ is used for rCBF evaluation at TMD1 or if $\frac{d}{dt}C(t)$ is used at TMD2, the correction factor can almost be ignored.

rCBF result obtained by MD1 andMD2 are more sensitive to local AIF

For a=3,4,5, $\frac{d}{dt}P(t,a)$=0.27, 0.224, 0.195 for MD1, so the error of the correction factor is around 17% for *a* between 3 and 4 and 13% for *a* between 4 and 5. So MD1 can be considered sensitive to the shape of AIF. The reason is that the correction factor for MD1 is proportional to the maximum value of AIF and the maximum values of local AIF's do not usually have similar values. The same large range of error appears for the correction factors $\frac{d^2}{dt}P(t,a)$ at TMD2, which are the correction factors for MD2.

Discussion

The recipe of finding correction factors is evaluating the results of $\int_0^t AIF(\tau)d\tau$. We have identified the different correction factors required for $C(t)$, MD1 and MD2 at rTOA's such as TMD1 and TMD2 and gave specific examples using the gamma-variate function as a model for AIF. Even though this manuscript presents only theoretical results, we brought up concerns over problems we might encounter in experimental data (e.g. $C(t)$ vs. MD1 and MD2 for rCBF estimation) when appropriate to provide an indication of the limitation of the theoretical model.

Is the rCBF result obtained by the maximum gradient based method relatively insensitive to local AIF, given the model of the gamma-variate function for AIF?

The relative insensitivity of $P(t, a)$ to *a* at t = TMD1 and of $\frac{d}{dt}P(t,a)$ to *a* at t = TMD2 suggests that under some special conditions of local AIF being coincidentally similar to normalized $e^{-t}t^{a-1}$, experimental data of $C(t)$ at TMD1 and $\frac{d}{dt}C(t)$ at TMD2 might also show low insensitivity to local AIF. We do not know how likely such special conditions for AIF would arise and we leave the question of whether the normalized gamma-variate function is the appropriate model for experimental AIF to other studies. On the other hand, since MD1 can be considered sensitive to the shape of AIF, the traditional maximum gradient method to

estimate perfusion, even under the "optimal" condition of AIF modeled by normalized $e^{-t}t^{a-1}$, would be sensitive to the effect of local AIF.

More comment on the generalized gamma-variate function model

In the more generalized gamma-variate function model for AIF, $S(t, a, b)$ yields the same correction factor of $P(t, a)$ at TMD1 if a is held constant, no matter how the value of b is varied. That also means that the results we obtained for $P(t, a)$ at TMD1 are translatable for $S(t, a, b)$ at TMD1. Hence we can safely ignore b and limit ourselves to varying the parameter a of $P(t, a)$ at TMD1. It is interesting to note that while the correction factor $S(t, a, b) = P(t, a)$ at TMD1 and TMD2, the results are however very different for the derivatives of $S(t, a, b)$ of $\frac{d}{dt}S(t,a,b)$ and $\frac{d^2}{dt}S(t,a,b)$

$$\frac{d}{dt}S(t,a,b)=b\frac{d}{dt}P(t,a) \text{ at TMD1 and at TMD2, and}$$
$$\frac{d^2}{dt}S(t,a,b)=b^2\frac{d^2}{dt}P(t,a) \text{ at TMD2}$$

So the correction factors for the generalized gamma-variate function model have a term dependent on b. Hence, if we pick two different AIF's which differ on the b value of the generalized gamma-variate model, correction factors for MD1 and MD2 could potentially be vastly different for the two AIF's. This is on top of the results reporting sensitivity for MD1 and MD2 to the variation in the value of a. It is fair to state that in varying either the a or the b parameters of the generalized gamma-variate model, the maximum gradient based method would be sensitive to the shape of local AIF. By contrast, estimating rCBF by $C(t)$ at TMD1 is relatively insensitive to both the a and the b parameters of the gamma-variate model of AIF.

Experimental data vs. simulation data

While we reported theoretical results on correction factors with simulation data, inevitable noise of experimental data could impose major constraints on the theoretical outcome. Below we discussed a number of factors likely to occur in experimental data.

A. Effect of miscalculation of rTOA on rCBF evaluation by ET—The proposal to estimate rCBF using MD1 at TMD1 and MD2 at TMD2 is a fairly robust way to estimate flow in ET, relatively independent of the error of estimated rTOA. MD1 remains relatively stable ranging from TMD1+1 to TMD1−1 while $C(t)$ could vary significantly in the same time range. Error in estimation of TMD1 could potentially compromise the accuracy of calculated rCBF more if $C(t)$ instead of MD1 is used for ET. Similar consideration applies to MD2 vs. $C(t)$. While $C(t)$, under the normalized gamma-variate function for AIF model, was shown to have some theoretical advantage over MD1 and MD2 in terms of sensitivity to local AIF, the robustness of MD1 and MD2 over $C(t)$ in the face of estimation error of TMD1 or TMD2 could be a more serious concern which must be taken into account in the application of ET.

How much error can we expect for rCBF given a miscalculation of rTOA if MD1 or MD2 are not used to evaluate rCBF? In the deconvolution literature, flow is known to be underestimated (Calamante et al., 2000; Ostergaard et al., 1996; Wu et al., 2003a) when time of arrival (TOA) of the tracer bolus is delayed relative to the arterial input function. The same type of underestimation in flow also occurs in ET (assuming either global AIF or known local AIF) when true TOA of the tracer bolus is delayed relative to the estimated TOA.

With regard to the degree of error to be expected in rCBF estimation, the proper response would be slightly more complicated in ET than in the deconvolution model. Since flow in the ET method can be estimated by a multiple number of ways (Kwong et al., 2011), each having its own strength and consideration (e.g. one can use the bolus time course $C(t)$, the integral of $C(t)$, derivative of $C(t)$, fractional derivatives of $C(t)$, etc), it is not possible to give a single blanket statement on how much mis-estimation of rCBF could occur. In general, the amount of rCBF error varies with the ET method applied. Specifically, the amount of rCBF error varies with the shape and size of the selected AIF and on the particular way AIF is used for the calculation of flow. This statement is true whether AIF is considered global or local. An explanation is given below.

If we estimate flow by $C(t)$, using TOA as the reference time point for ET, flow f is shown in Eq (4) of the Introduction Section above to be

$$C(t) \approx f\int_0^t AIF(\tau)d\tau \quad or$$
$$f \approx \frac{c(t)}{\int_0^t AIF(\tau)d\tau}$$

The flow ratio of two different pixels in ET is *independent* of AIF(t) if we assume global AIF, but the *amount of flow error* coming from the mis-estimation of TOA, based on Eq (4), would be *dependent* on t and on the shape and size of the particular AIF(t). Therefore, one cannot evaluate "how much effect of the delay of the bolus on rCBF estimate" without a good knowledge of the specific AIF(t).

Similarly, if flow is estimated by $\frac{d}{dt}C(t)$ instead,

$$f \approx \frac{\frac{d}{dt}C(t)}{AIF(t)}$$

and the amount of error in estimated f due to error in TOA would be different from the error obtained using Eq (4), but would still again depend on the shape and size of AIF(t).

In the local AIF model, it means that the assessment of error in flow would depend on the adequacy of the local AIF identification. The same argument goes with the use of other forms of derivatives of $C(t)$ to evaluate flow errors associated with misestimated TOA.

B. Effect of contrast agent leakage on rCBF estimation by ET—ET assumes that the contrast agent has no chance to leave from the tissue. Is there a way to account for clinical patients who show leakage of contrast agent?

"How much" leakage effect is there on rCBF estimation by ET? The simple answer is: it could range from none to very little. Below we will give a more detailed answer.

rCBF evaluation by ET (or by deconvolution) is not expected to be affected by leakage in the following applications: In computed tomography (CT) perfusion analysis with a first pass bolus (Aviv et al., 2009; Bisdas et al., 2007; Cenic et al., 2000; Koh et al., 2006; Nabavi et al., 1999), in T1 based MRI Dynamic Contrast-enhanced (DSC-MRI) first pass study (Larsson et al., 2009), in PET perfusion (Larson et al., 1987) of the distributed parameter models where radiolabeled water is not 100% freely diffusive and retains a vascular component. The reason is that given the assumption of $R(t) = 1$ before the tissue

mean transit time, the external image detector, as explained by Larson et al. (Larson et al., 1987) cannot distinguish between tracer extracted into tissue and tracer in blood, but instead registers a response proportional to the total amount of tracer in the injected bolus.

While the evaluation of relative cerebral blood volume (rCBV) would be affected by the leakage (Axel, 1980; Cenic et al., 1999), such discussion will be deferred as our current manuscript is limited to ET on rCBF.

In T2* based DSC-MRI, on the other hand, a model has been presented to correct the bolus concentration time course of the effects of T1 changes associated with the leaks of gado agents (Donahue et al., 2000; Quarles et al., 2005; Weisskoff et al., 1994). In principle, once the experimental bolus concentration time course is successfully modified, corrected rCBF result can be obtained independent of which perfusion analysis method (e.g. deconvolution or ET) is employed.

In practice, in the literature of the deconvolution approach, rCBF was rarely corrected in T2* based DSC-MRI. The correction of the concentration time curve was directed mainly to the effect on rCBV (Boxerman et al., 2006; Covarrubias et al., 2004; Donahue et al., 2000; Paulson and Schmainda, 2008; Quarles et al., 2005). The reason is that the T1 effect due to leakage would be the strongest late at the tail end of the bolus signal, leading to inaccurate assessment of rCBV values. rCBF results which depend overwhelmingly on the early time points are hardly affected, a consideration applicable to ET as well as the deconvolution method. While we can always choose to apply a model to correct any T1 effect on the experimental T2* based concentration time course, the simple argument is, even without any modeling, that the total amount of leakage is small at the early time points, leading to a small T1 effect on the bolus data signal and can be reasonably ignored in ET for rCBF evaluation.

One may ask whether the range of “early time points” is consistent with the assumption of a small amount of leakage. What would be an upper time point boundary for “early time points” of ET? We know, as explained in our companion paper on fractional derivatives, that ET basic assumption would fail before $C(t)$ reaches its peak (has ET always held, $C(t)$ would plateau and not turn back at its peak). But that is just the upper limit. Literature shows (Klotz and Konig, 1999; Miles and Griffiths, 2003) that it is feasible for ET to also fail before TMD1. So “early time points” consistent with ET really encompass just the early rising part of the bolus time curve where change of T2* and T1 would be insignificant, as shown from the lack of difference between the uncorrected and corrected mean rCBF values given in (Quarles et al., 2005).

Strictly speaking, the T1 effect of leaked gado agents becomes a problem for T2* based DSC-MRI mainly because the bolus concentration is calculated as $\Delta R2^*(t)=\frac{-1}{TE}\ln\left(\frac{S(t)}{S_o}\right)$ where $\Delta R2^*(t)$ is the change in transverse relaxivity for gradient echo, $S(t)$ is the signal intensity of a single echo MR sequence at time t, S_0 is the baseline signal intensity before the bolus arrives. Had the concentration time course been converted from the difference of $R2^*(t)$ obtained from fitting the signal decay of a multi-echo gradient echo sequence, the T1 effect would not play a role. Here we assume that $\Delta R2^*(t)$ is the same whether the contrast agent is in the vessels or has leaked out. It is an assumption made by virtually all the current T2* based DSC-MRI models (Donahue et al., 2000; Johnson et al., 2004) but with the acknowledgement that details of the assumption remain to be investigated (Zaharchuk, 2007). There is also the first-pass T2* method or first-pass parametric model of Johnson et al. (Johnson et al., 2004) with the authors claiming that they had never observed any marked T1 effect in leaky tumors. If one accepts the claim on T1 by Johnson et al. or if $\Delta R2^*(t)$ can be obtained from a multi-echo sequence, the estimation of rCBF by ET using T2* DSC-MRI

data would again be independent of leakage just like the CT perfusion analysis presented earlier. Also as mentioned above, leakage does affect the evaluation of rCBV which, while it is not immediately relevant to our discussion on ET, could be evaluated by a large number of published methods, including many of citations listed above.

C. Future considerations for a comparison of theoretical model vs. experimental data—We chose to focus on presenting only a theoretical model here and not including a comparison of experimental data. Numerous confounding factors of experimental data such as the effect of the random noise and physiological noise, the multiple transit times of the partial volumed experimental signal vs. the single transit time model in simulation, and the additional unknowns of the quality of the local AIF model, are all considerations that make a non-trivial comparison between the theoretical model and experimental data beyond the scope of the current manuscript. What is required for setting up a future comparison of the experimental data with some of the specific claims of the theoretical model? We can consider the example of one specific claim mentioned in the manuscript: Is experimental rCBF result obtained by $C(t)$ at TMD1 really (relatively) insensitive to local AIF? Before the claim can be evaluated, we need to have a "gold standard" of perfusion values to identify experimental pixels which have "truly" equal flow values. Such a "gold standard" can be obtained by measuring flow using a microsphere model in future animal experiments.

We believe that clarifying the different theoretical aspects of the correction factors in this current manuscript is of sufficient relevance and utility for the perfusion research community. Future research will be needed for a more detailed evaluation of experimental data in the ET context for local AIF.

Second Recipe

We have provided a recipe to find the correction factors based on local AIF. Other recipes are available but they all depend on the same principle of taking into account the different shapes of the AIF's. For reference, a second recipe is also described at the Supplementary Material section together with the graphical illustration of Fig. S1.

Conclusion

Given the information of local AIF, proper correction factors can be obtained for ET to evaluate rCBF based on the microsphere perfusion model. If $C(t)$ is used for rCBF calculation, the correction factor is a normalized integral of the local AIF up to any early time point of our choice. In the special cases of using MD1 and MD2 for rCBF estimation, the correction factor is the maximum signal of AIF for MD1 and the maximum first derivative of AIF for MD2.

Supplementary Material

Refer to Web version on PubMed Central for supplementary material.

Acknowledgments

We would like to acknowledge the support of the Athinoula A. Martinos Center for Biomedical Imaging.

Glossary

AIF arterial input function

***C*(*t*)**	tissue contrast agent bolus concentration time curve
ET	early time points perfusion imaging method
MD1	maximum derivative of *C*(*t*)
MD2	maximum second derivative of *C*(*t*)
***P*(*t*,*a*)**	the incomplete lower gamma function
rTOA	relative time of arrival of the contrast agent bolus
T	tissue mean transit time
TMAIF	time to reach the maximum signal of AIF
TMD1	time to reach the maximum derivative
TMD2	time to reach the maximum second derivative
TOA	time of arrival of the contrast agent bolus

References

Aviv RI, d'Esterre CD, Murphy BD, Hopyan JJ, Buck B, Mallia G, Li V, Zhang L, Symons SP, Lee TY. Hemorrhagic transformation of ischemic stroke: prediction with CT perfusion. Radiology. 2009; 250:867–877. [PubMed: 19244051]

Axel L. Cerebral blood flow determination by rapid-sequence computed tomography: theoretical analysis. Radiology. 1980; 137:679–686. [PubMed: 7003648]

Bisdas S, Hartel M, Cheong LH, Koh TS, Vogl TJ. Prediction of subsequent hemorrhage in acute ischemic stroke using permeability CT imaging and a distributed parameter tracer kinetic model. J Neuroradiol. 2007; 34:101–108. [PubMed: 17383003]

Boxerman JL, Schmainda KM, Weisskoff RM. Relative cerebral blood volume maps corrected for contrast agent extravasation significantly correlate with glioma tumor grade, whereas uncorrected maps do not. AJNR Am J Neuroradiol. 2006; 27:859–867. [PubMed: 16611779]

Buxton, RB. Introduction to Functional Magnetic Resonance Imaging, Principles and Techniques. Cambridge University Press; 2002. Perfusion Imaging, Contrast Agent Techniques; p. 342

Calamante F. Bolus dispersion issues related to the quantification of perfusion MRI data. J Magn Reson Imaging. 2005; 22:718–722. [PubMed: 16261569]

Calamante F, Gadian DG, Connelly A. Delay and dispersion effects in dynamic susceptibility contrast MRI: simulations using singular value decomposition. Magn Reson Med. 2000; 44:466–473. [PubMed: 10975900]

Calamante F, Morup M, Hansen LK. Defining a local arterial input function for perfusion MRI using independent component analysis. Magn Reson Med. 2004; 52:789–797. [PubMed: 15389944]

Cenic A, Nabavi DG, Craen RA, Gelb AW, Lee TY. Dynamic CT measurement of cerebral blood flow: a validation study. AJNR Am J Neuroradiol. 1999; 20:63–73. [PubMed: 9974059]

Cenic A, Nabavi DG, Craen RA, Gelb AW, Lee TY. A CT method to measure hemodynamics in brain tumors: validation and application of cerebral blood flow maps. AJNR Am J Neuroradiol. 2000; 21:462–470. [PubMed: 10730636]

Covarrubias DJ, Rosen BR, Lev MH. Dynamic magnetic resonance perfusion imaging of brain tumors. Oncologist. 2004; 9:528–537. [PubMed: 15477637]

Donahue KM, Krouwer HG, Rand SD, Pathak AP, Marszalkowski CS, Censky SC, Prost RW. Utility of simultaneously acquired gradient-echo and spin-echo cerebral blood volume and morphology maps in brain tumor patients. Magn Reson Med. 2000; 43:845–853. [PubMed: 10861879]

Herfkens RJ, Axel L, Lipton MJ, Napel S, Berninger W, Redington R. Measurement of cardiac output by computed transmission tomography. Invest Radiol. 1982; 17:550553.

Johnson G, Wetzel SG, Cha S, Babb J, Tofts PS. Measuring blood volume and vascular transfer constant from dynamic, T(2)*-weighted contrast-enhanced MRI. Magn Reson Med. 2004; 51:961–968. [PubMed: 15122678]

Kimura T, Kusahara H. Reference-based maximum upslope: a CBF quantification method without using arterial input function in dynamic susceptibility contrast MRI. Magn Reson Med Sci. 2009; 8:107–120. [PubMed: 19783874]

Klotz E, Konig M. Perfusion measurements of the brain: using dynamic CT for the quantitative assessment of cerebral ischemia in acute stroke. Eur J Radiol. 1999; 30:170–184. [PubMed: 10452715]

Koenig M, Klotz E, Luka B, Venderink DJ, Spittler JF, Heuser L. Perfusion CT of the brain: diagnostic approach for early detection of ischemic stroke. Radiology. 1998; 209:85–93. [PubMed: 9769817]

Koh TS, Cheong LH, Tan CK, Lim CC. A distributed parameter model of cerebral blood-tissue exchange with account of capillary transit time distribution. Neuroimage. 2006; 30:426–435. [PubMed: 16246589]

Kwong KK, Chan ST, Wu O, Nelissen K, Chesler DA. Early Time Points Perfusion Imaging: Relative Time of Arrival, Maximum Derivatives and Fractional Derivatives. (companion paper).

Kwong KK, Reese TG, Nelissen K, Wu O, Chan ST, Benner T, Mandeville JB, Foley M, Vanduffel W, Chesler DA. Early time points perfusion imaging. Neuroimage. 2011; 54:1070–1082. [PubMed: 20851196]

Larson KB, Markham J, Raichle ME. Tracer-kinetic models for measuring cerebral blood flow using externally detected radiotracers. J Cereb Blood Flow Metab. 1987; 7:443–463. [PubMed: 3611204]

Larsson HB, Courivaud F, Rostrup E, Hansen AE. Measurement of brain perfusion, blood volume, and blood-brain barrier permeability, using dynamic contrast-enhanced T(1)- weighted MRI at 3 tesla. Magn Reson Med. 2009; 62:1270–1281. [PubMed: 19780145]

Lorenz C, Benner T, Chen PJ, Lopez CJ, Ay H, Zhu MW, Menezes NM, Aronen H, Karonen J, Liu Y, Nuutinen J, Sorensen AG. Automated perfusion-weighted MRI using localized arterial input functions. J Magn Reson Imaging. 2006a; 24:1133–1139. [PubMed: 16969793]

Lorenz C, Benner T, Lopez CJ, Ay H, Zhu MW, Aronen H, Karonen J, Liu Y, Nuutinen J, Sorensen AG. Effect of using local arterial input functions on cerebral blood flow estimation. J Magn Reson Imaging. 2006b; 24:57–65. [PubMed: 16767708]

Miles KA. Measurement of tissue perfusion by dynamic computed tomography. Br J Radiol. 1991; 64:409–412. [PubMed: 2036562]

Miles KA, Griffiths MR. Perfusion CT: a worthwhile enhancement? Br J Radiol. 2003; 76:220–231. [PubMed: 12711641]

Nabavi DG, Cenic A, Craen RA, Gelb AW, Bennett JD, Kozak R, Lee TY. CT assessment of cerebral perfusion: experimental validation and initial clinical experience. Radiology. 1999; 213:141–149. [PubMed: 10540654]

Ostergaard L, Weisskoff RM, Chesler DA, Gyldensted C, Rosen BR. High resolution measurement of cerebral blood flow using intravascular tracer bolus passages. Part I: Mathematical approach and statistical analysis. Magn Reson Med. 1996; 36:715–725. [PubMed: 8916022]

Paulson ES, Schmainda KM. Comparison of dynamic susceptibility-weighted contrast- enhanced MR methods: recommendations for measuring relative cerebral blood volume in brain tumors. Radiology. 2008; 249:601–613. [PubMed: 18780827]

Quarles CC, Ward BD, Schmainda KM. Improving the reliability of obtaining tumor hemodynamic parameters in the presence of contrast agent extravasation. Magn Reson Med. 2005; 53:1307–1316. [PubMed: 15906288]

Weisskoff, RM.; Boxerman, JL.; Sorensen, AG.; Kulke, S.; Campbell, T.; Rosen, BR. Simultaneous blood volume and permeability mapping using a single Gd-based contrast injection. Proceedings of the Twelfth Annual Meeting of the Society for Magnetic Resonance Imaging; San Francisco. 1994. p. 279

Willats L, Connelly A, Calamante F. Improved deconvolution of perfusion MRI data in the presence of bolus delay and dispersion. Magn Reson Med. 2006; 56:146–156. [PubMed: 16767744]

Willats L, Connelly A, Calamante F. Minimising the effects of bolus dispersion in bolus-tracking MRI. NMR Biomed. 2008; 21:1126–1137. [PubMed: 18727165]

Wu O, Ostergaard L, Koroshetz WJ, Schwamm LH, O'Donnell J, Schaefer PW, Rosen BR, Weisskoff RM, Sorensen AG. Effects of tracer arrival time on flow estimates in MR perfusion-weighted imaging. Magn Reson Med. 2003a; 50:856–864. [PubMed: 14523973]

Wu O, Ostergaard L, Weisskoff RM, Benner T, Rosen BR, Sorensen AG. Tracer arrival timing-insensitive technique for estimating flow in MR perfusion-weighted imaging using singular value decomposition with a block-circulant deconvolution matrix. Magn Reson Med. 2003b; 50:164–174. [PubMed: 12815691]

Zaharchuk G. Theoretical basis of hemodynamic MR imaging techniques to measure cerebral blood volume, cerebral blood flow, and permeability. AJNR Am J Neuroradiol. 2007; 28:1850–1858. [PubMed: 17998415]

Research Highlights

Correction factors for rCBF measurement by ET are derived from the integral of AIF. In some special settings of the gamma variate model of AIF, correction factors may almost be ignored. Sources of error for rCBF estimation of experimental data are reviewed in the Discussion Section.

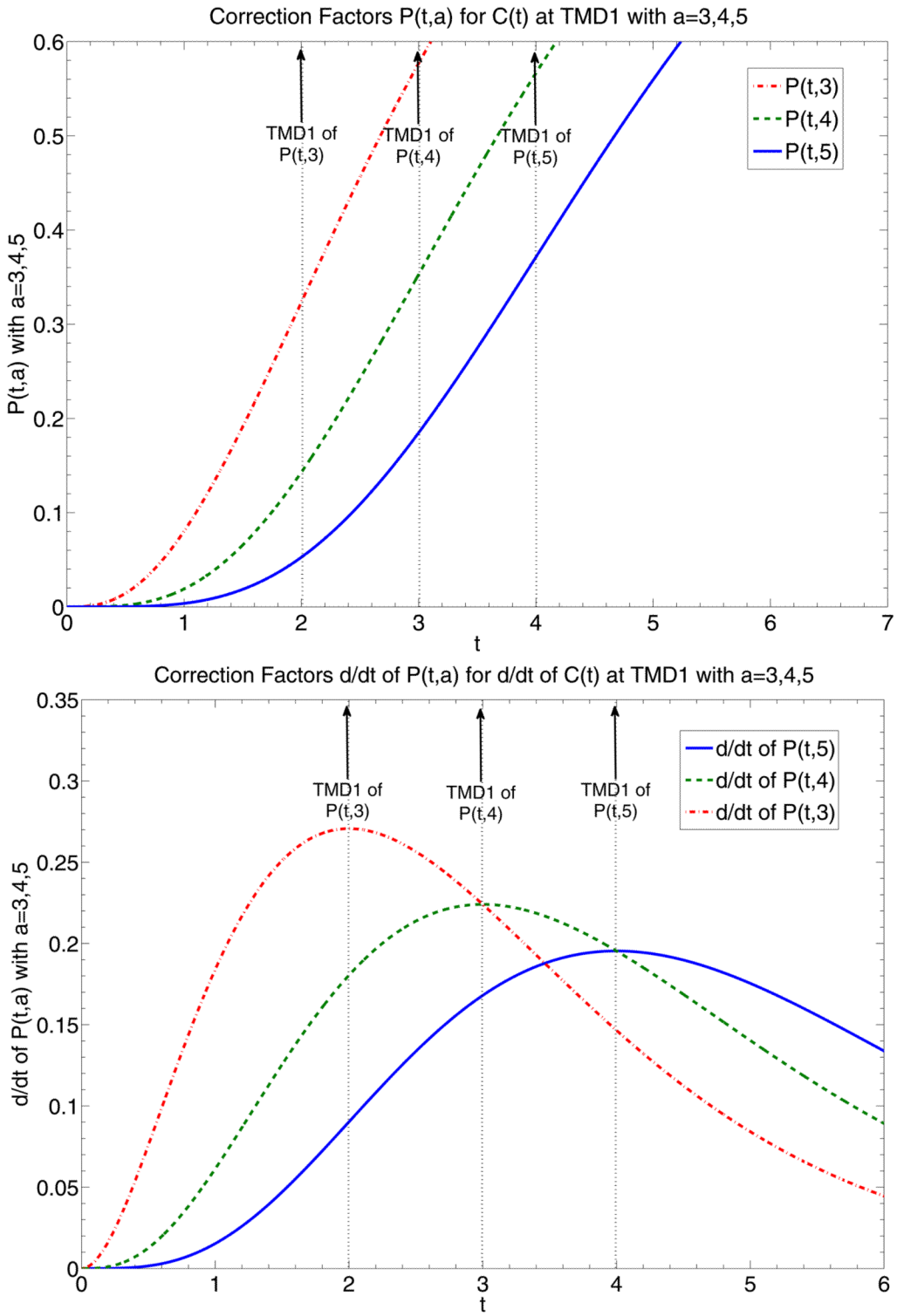

Fig. 1.

(a) Graphs of $P(t, 3)$, $P(t, 4)$ *and* $P(t, 5)$, representing correction factors of $C(t)$ given different local AIF's modeled by normalized $e^{-t}t^{a-1}$ with parameter a equal to 3, 4, and 5. Dotted vertical lines highlight the time points of TMD1 of $P(t, 3)$, $P(t, 4)$ *and* $P(t, 5)$.

Intersection of dotted vertical lines with graphs of $P(t, 3)$, $P(t, 4)$ *and* $P(t, 5)$ return correction factor values of $C(t)$ at TMD1, correction factor values equal to 0.323, 0.353 and 0.371, which are relatively close to each other. **(b)** Graphs of $\frac{d}{dt}P(t,3)$, $\frac{d}{dt}P(t,4)$ and $\frac{d}{dt}P(t,5)$, representing correction factors of $\frac{d}{dt}C(t)$ and equivalent to the respective AIF's. Dotted vertical lines highlight the time points of TMD1 of $P(t, 3)$, $P(t, 4)$ *and* $P(t, 5)$ which are equivalent to the time points of the maximum signal of the respective AIF's. Intersection of dotted vertical lines with graphs of $\frac{d}{dt}P(t,3)$, $\frac{d}{dt}P(t,4)$ and $\frac{d}{dt}P(t,5)$ return the correction factor values of $\frac{d}{dt}C(t)$ at TMD1, or equivalently MD1, values equal to 0.27, 0.224 and 0.195, which are not as close to each other as those presented in (a).

Table 1

Correction Factor

The values of correction factors based on $P(t, a)$ are listed for t =TMD1 and t =TMD2. The correction factor for $C(t)$ is $P(t, a)$. The correction factor for $\frac{d}{dt}C(t)$ is $\frac{d}{dt}P(t,a)$. The correction factor for $\frac{d^2}{dt}C(t)$ is $\frac{d^2}{dt}P(t,a)$. The following results are reported by Table 1: The correction factors for the signal intensity at TMD1 and for the first derivative value at TMD2 are relatively insensitive to the value a, or equivalently the shape of the gamma-variate function AIF. In contrast, correction factors for the first derivative at TMD1 and the second derivative at TMD2 are more sensitive to a. The second derivative of $C(t)$ at TMD1 is naturally zero so the correction factor $\frac{d^2}{dt}P(t,a)$ is also zero at TMD1.

t	**Value *a* of *P*(*t*, *a*)**	**Correction Factor P(t, a) for Signal Intensity of tissue curve**	**Correction Factor $\frac{d}{dt}P(t,a)$ for first Derivative of tissue curve**	**Correction Factor $\frac{d^2}{dt}P(t,a)$ for second Derivative of tissue curve**
TMD1	3	0.3233	0.2707	0
	4	0.3528	0.2240	0
	5	0.3712	0.1954	0
TMD2	3	0.02174	0.0955	0.2306
	4	0.04	0.0956	0.1306
	5	0.05265	0.0902	0.0902